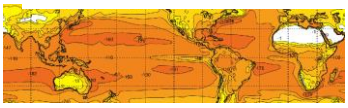

Upgrading and Estimation of Long Time Series of Heat Fluxes from Remotely Sensed Observations.
1992 - 2018

Report prepared by Dr Abderrahim Bentamy. OHF Project coordinator

Institut Français pour la Recherche et l'Exploitation de la MER (IFREMER) / Centre Bretagne
Laboratoire d'Océanographie Physique et Spatial (LOPS)

Contacts
abderrahim.bentamy@ifremer.fr
antoine.grouazel@ifremer.fr
jean.francois.piolle@ifremer.fr

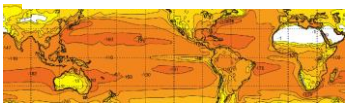

Abstract

This documents reports the latest improvements dealing with the determination, data extension, and validation of heat fluxes and the related bulk variables over the global oceans at regular spatial grid of 0.25° in latitude and longitude. The new version products are available as daily and monthly averaged estimates.

In 2018, Ifremer made available long time series (1992 – 2016) of daily turbulent fluxes, referenced as version 4 (V4). The latter is updated and extended through December 31st 2018. The main changes with respect to version 4 (V4) rely on the enhancements of the empirical model relating satellite brightness temperature measurements and the specific air humidity at 10m height (Q_{a10}), and on the use of extended and updated remotely sensed wind speeds.

Data are available through ftp.

ftp://o1ef56@eftp.ifremer.fr/oceanheatflux/data/third-party/fluxes/ifremerflux_v4.1_daily/
ftp://o1ef56@eftp.ifremer.fr/oceanheatflux/data/third-party/fluxes/ifremerflux_v4.1_monthly/

1 Overview

The European Space Agency (ESA) Ocean Heat Flux (OHF) (https://wwz.ifremer.fr/oceanheatflux/) project provided useful and powerful tools for assessing the quality of heat fluxes (latent and sensible heat fluxes), and of the related bulk variables (wind speed, zonal and meridional wind vector components, surface and air temperatures, and surface and air specific humidities). The main results can be found in OHF progress reports and handbook. The related main scientific results are in (Bentamy *et al*, 2017a). For instance, it was shown that though Ifremer fluxes compare well to mooring daily estimates, they exhibit lower results over some specific regions such as western boundary currents: Gulf Stream and Kurishio. Ifremer fluxes tend to be underestimated for high heat flux conditions. The underestimation is mostly due to specific air humidity and on wind speed issues (Bentamy *et al*, 2017a)

This new version of Ifremer daily heat fluxes uses the updated empirical model relating 10m specific air humidity (Q_{a10}) and radiometer brightness temperature (*TB*) measurements. The determination of the empirical Q_{a10} model is described in (Bentamy *et al*, 2013). For this project, a new calibration of Q_{a10} *model* is performed in conjunction with the use of the recently

re-processed fundamental climate data record (FCDR) of brightness temperatures from the Colorado State University (CSU_FCDR) (Wesley *et al*, 2013), and the latest reprocessed International Comprehensive Ocean–Atmosphere Data Set (ICOADS Version 3; Freeman *et al*. 2017). The latter is a compilation of in situ surface marine observations (ship, moored and drift buoys). ICOADS Q_{a10} and FCDR_CSU *TB* are collocated in space and time. The resulting collocated data allow the determination and improvement of the satellite Q_{a10} model. Figure 1 shows examples of monthly mean difference between Q_{a10} from OHF standard product (Bentamy *et al* 2017a) and from the updated estimates. The former are calculated from daily estimates occurring in January (Figure 1a) and July (Figure 1b) 2003. The main departure between the two estimates are clearly depicted in Gulf Stream, Kurishio, and Aghulas regions, where the OHF standard data are overestimated compared to the new data. Such overestimation leads to the underestimation of OHF standard LHF (Bentamy *et al*, 2017a).

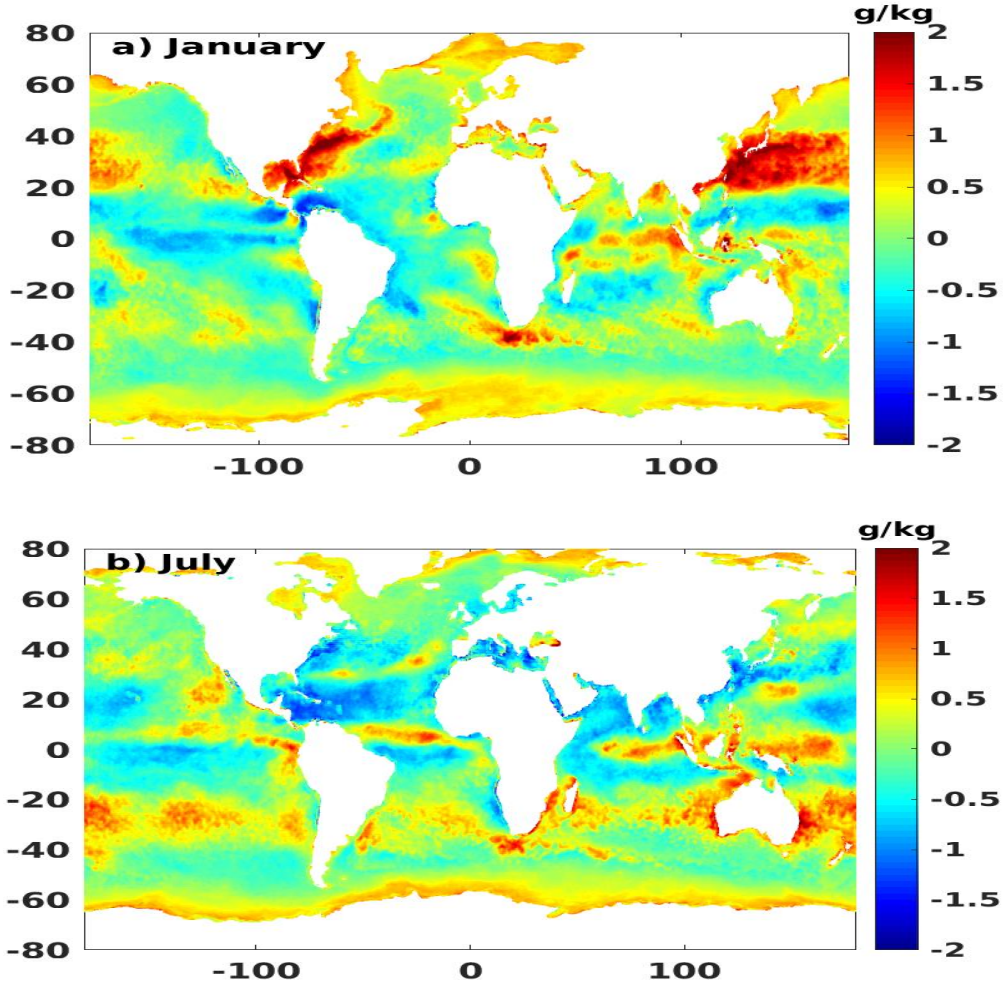

Figure 1: Monthly mean differences of standard OHF Ifremer minus new Ifremer specific humidity (Q_{a10}) products, estimated from a) January and b) July 2003 dally data

To achieve the extension of the long time series through end of 2018, FCDR TB data from remote sensing system (FCDR_RSS) (Wentz et al, 2013) are used. Indeed FCDR_CSU are only available along the period 1992 – June 2017. FCDR_RSS are used for the determination of Q_{a10}, based on the aforementioned empirical mode, along the period June 2017 – December 2018. Figure 2 shows comparison of Q_{a10} estimated from FCDR_CSU and from FCR_RSS *TB* occurring in June 2017. The mean difference (Figure 2a) between the two retrievals is almost negligible, expect at some nearcoast locations. The related standard deviation (Figure 2b) is mostly lower than 0.35g/kg. Obviously no systematic departure between the Q_{a10} retrievals is found.

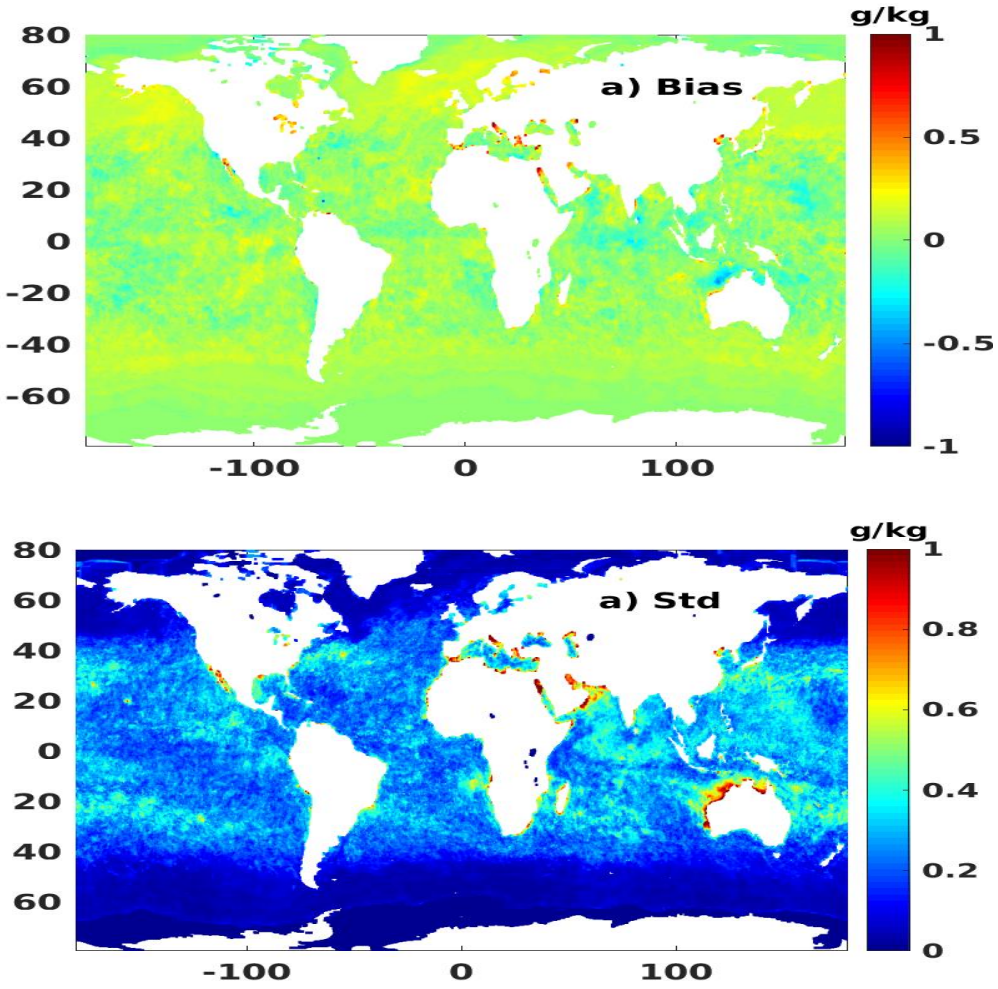

Figure 2: Mean (top) and related standard deviation (STD) (Bottom) of difference between Q_{a10} retrieved from FCDR_CSU and FCDR_RSS TB occurring in June 2017.

To further assess the impact of the use RSS *TB* for extending the time series of turbulent heat fluxes, LHF calculated based on the use of CSU and RSS *TB* occurring in June 2017 are

compared over the Atlantic, Pacific, and Indian Oceans (Figure 3). The two LHF estimates track each other closely. The main departures are found at high latitudes, but are not statistically significant at 95% confident.

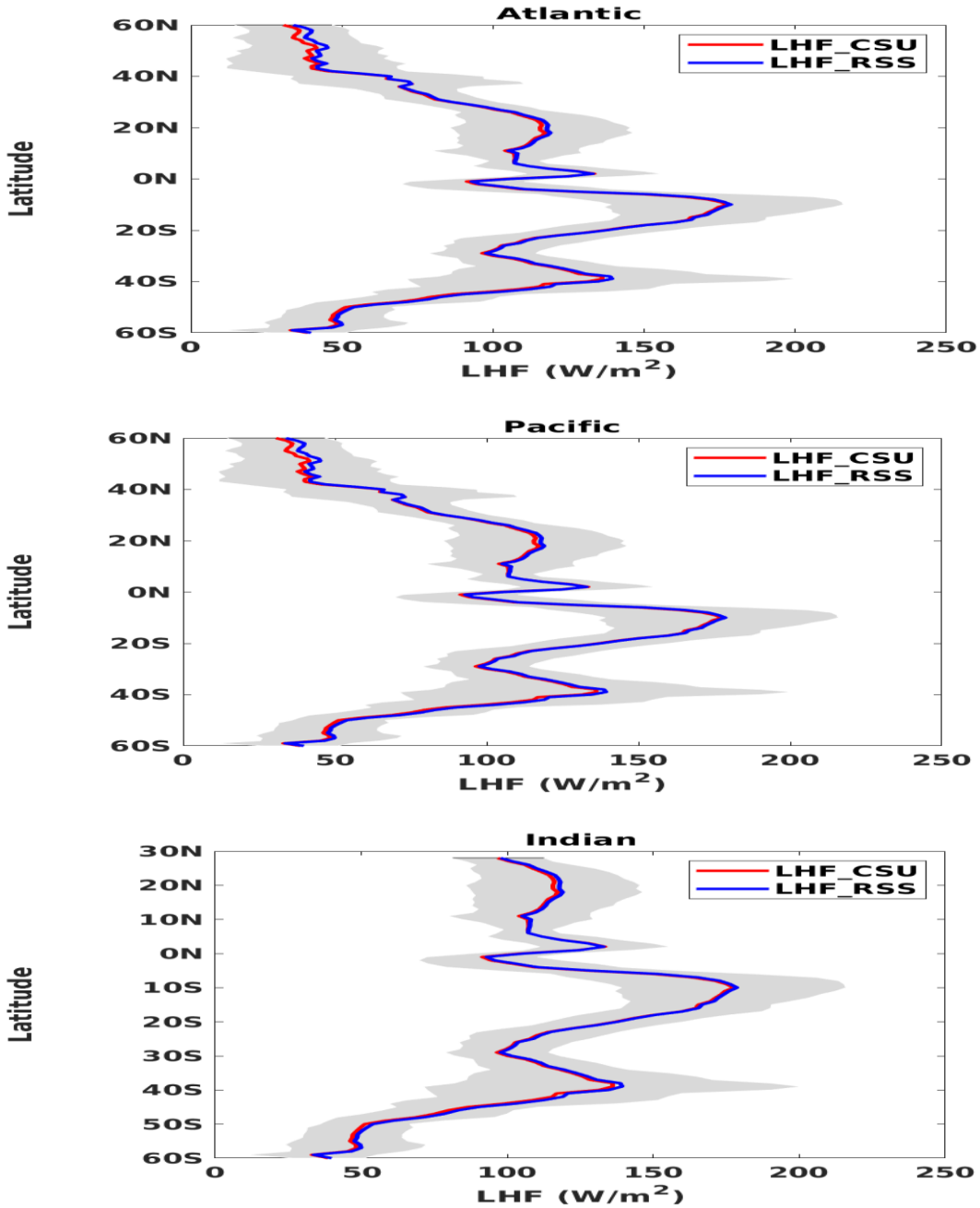

Figure 3: Latitudinal means of LHF estimated based on the use of CSU (LHF_CSU in red color) and RSS (LHF_RSS in blue color) brightness temperatures. Grey zone indicates one standard deviation variation of LHF_CSU.

The reprocessing of long time series of turbulent fluxes uses wind retrievals from all scatterometers available during the period 1992 – 2018. Radiometers wind retrievals are also used as ancillary data. Scatterometer data are provided by IFREMER (ERS-1 and ERS-2), NASA/JPL (NSCAT, QuikSCAT, SeaWinds, and RapidScat), EUMETSAT OSI (ASCAT-A and ASCAT-B), CNSA (HY-2A), ISRO (OceanSat-2). Radiometer winds are from Remote Sensing System (SSM/I SSMIS, and WindSat). The new Ifremer flux version uses the inter-calibrated scatterometer wind retrievals as described in (Bentamy *et al*, 2017b).

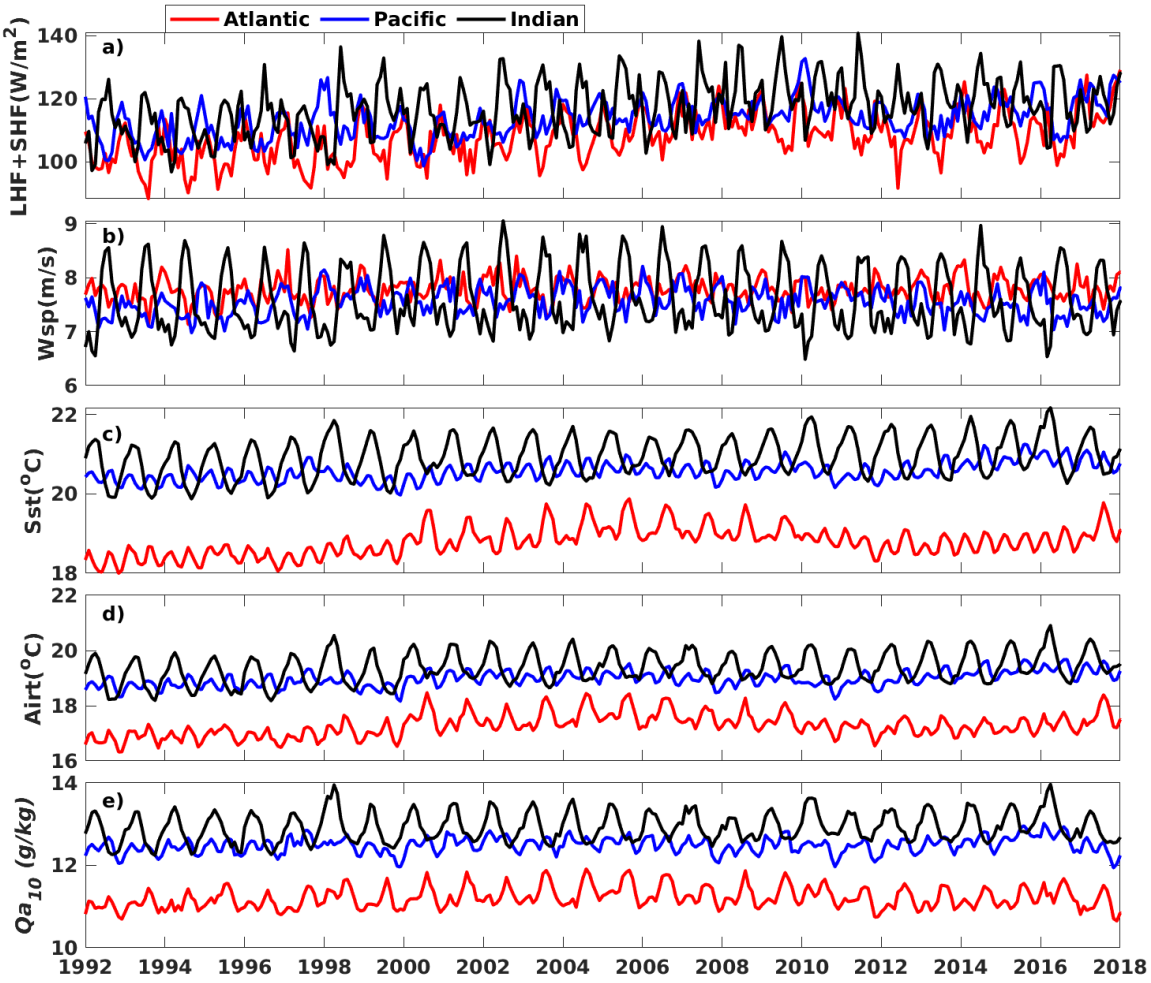

Figure 4: Time series (January 1992 – December 2018) of regional means of a) LHF+SHF , b) 10m wind speed(Wsp), c) Sst, d) Air temperature (Airt), and e) Qa10. Red, blue, and black colors indicate means estimated over the Atlantic, Pacific, and Indian Oceans, respectively.

The time series of the main resulting variables of the new OHF Ifremer product are illustrated in Figure 4. It shows monthly means estimated over the Atlantic, Pacific, and Indian Oceans from monthly-averaged data along the period January 1992 through December 2018. Figures 5 and 6 illustrate the seasonal distributions of latent and sensible heat fluxes over the global oceans, respectively. They are estimated for Northern hemisphere seasons winter (December, January, February (DJF)), spring (March, April, May (MAM)), summer (June, July, August (JJA)), and fall (September, October, November (SON)).

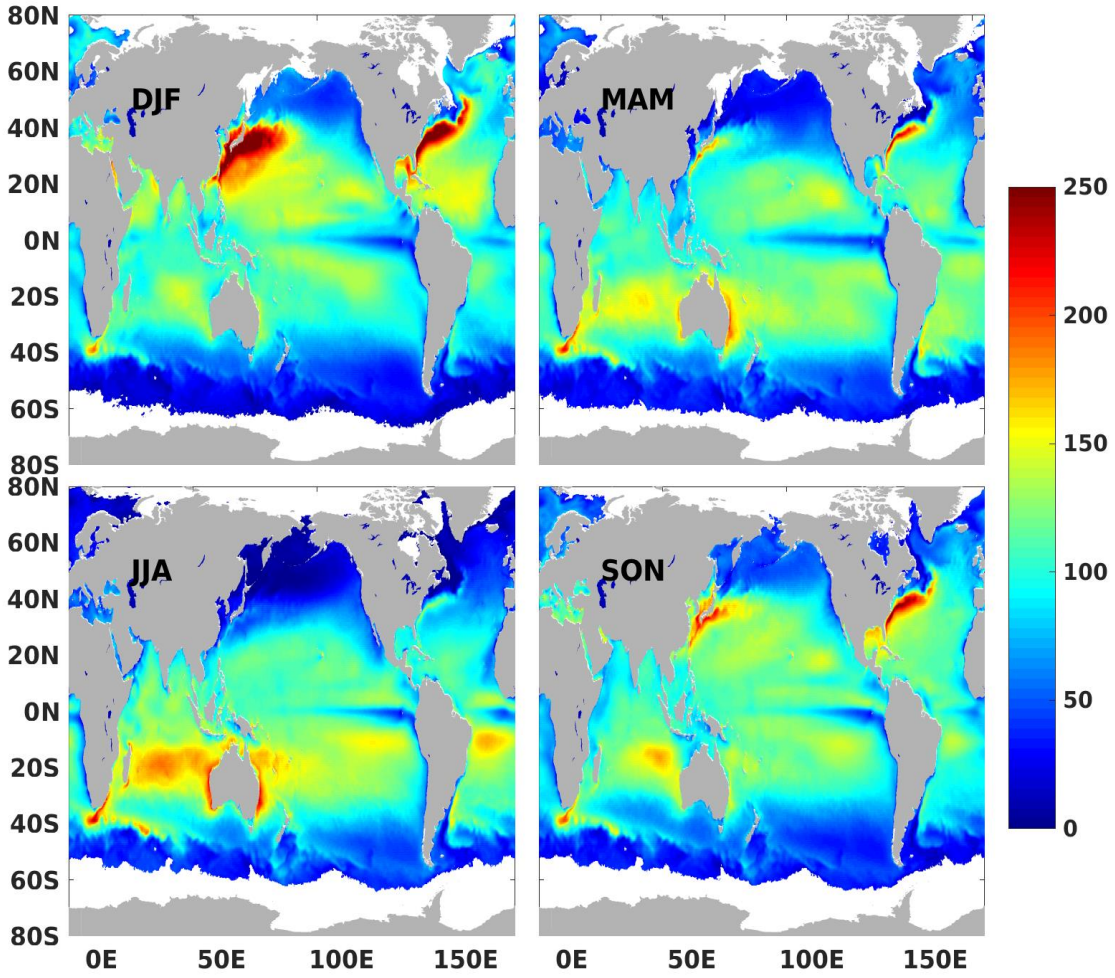

Figure 5: Seasonal latent heat flux distributions estimated from Ifremer daily LHF (1992 – 2018). Color indicates LHF values in (W/m²)

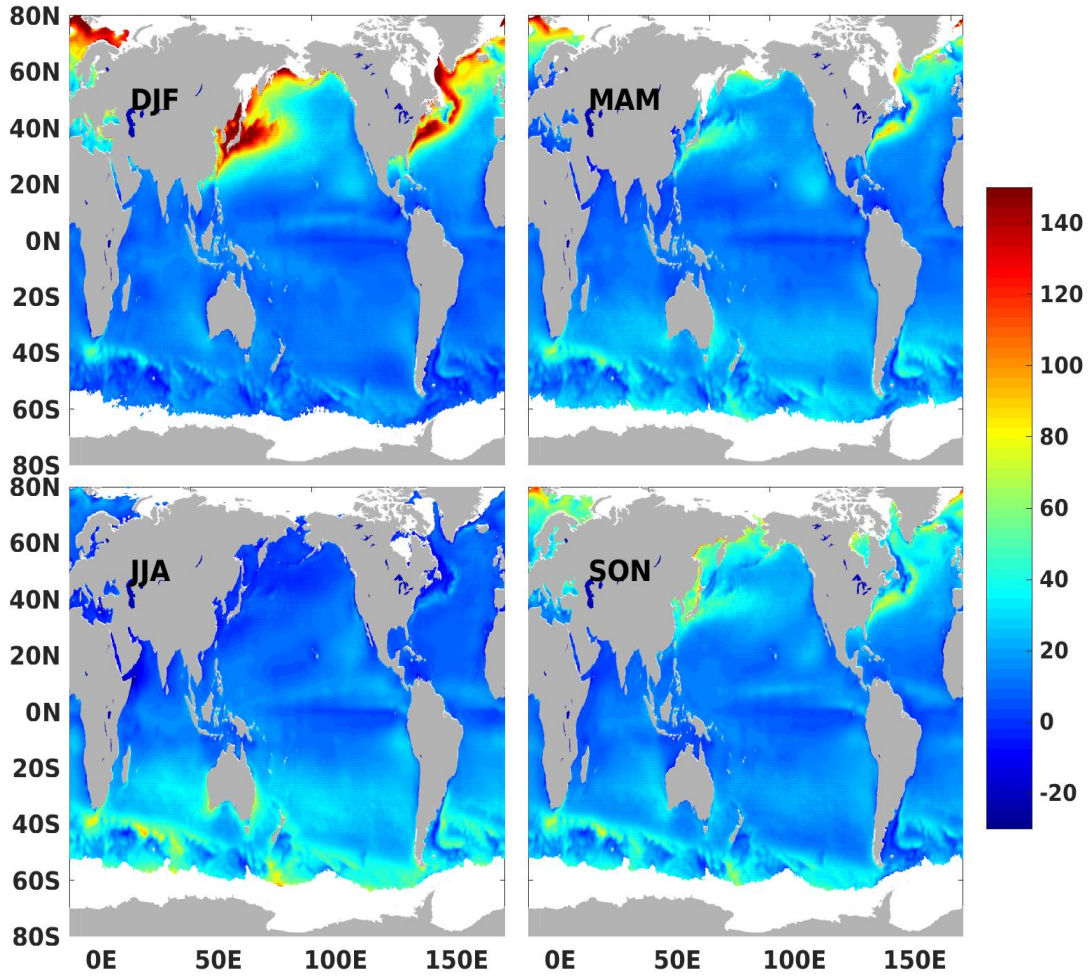

Figure 6: Seasonal sensible heat flux distributions estimated from Ifremer daily SHF (1992 – 2018). Color indicates SHF values in (W/m²)

2 Accuracy Issues

The accuracy of the newest Ifremer fluxes is determined through comprehensive comparisons with daily buoy latent and sensible heat flux estimates. The full description of buoy flux determination is provided in (Bentamy *et al*, 2017a). Figure 7 shows buoy locations.

Table 1 shows statistic parameters illustrating the comparisons between satellite and buoy daily latent and sensible heat fluxes. The former assess the good agreement between buoy and Ifremer heat fluxes and bulk variables.

As expected, the accuracy results may vary seasonally and with respect to buoy location, as discussed in (Bentamy *et al*, 20017a). Figures 8 shows the RMSD and correlation of buoy and satellite-based LHF SHF at each buoy location. Similar SHF results are shown in Figure 9.

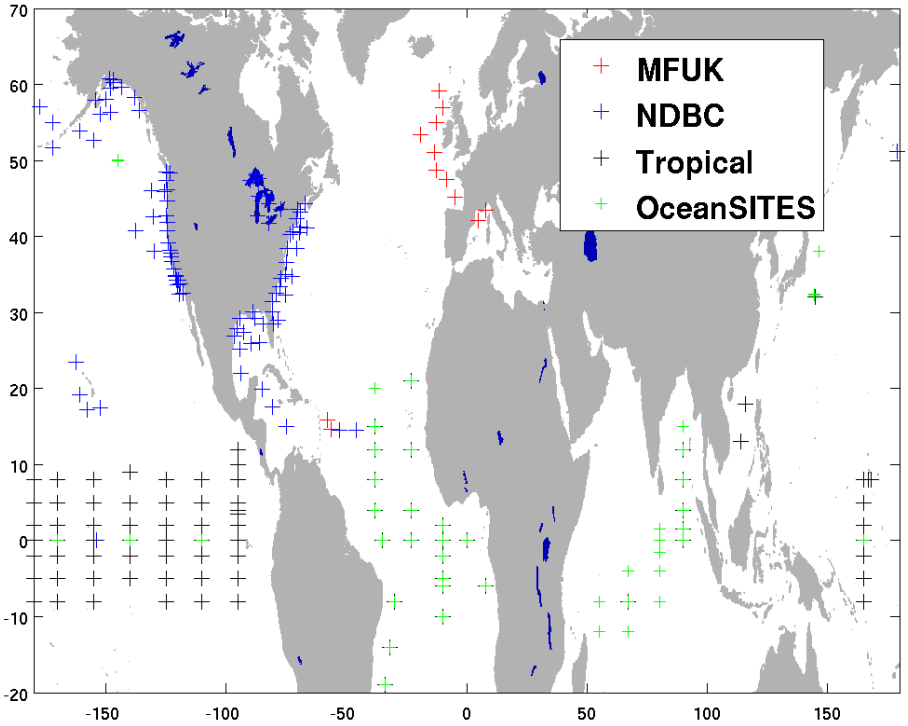

Figure 7: Moored buoy Locations. Red, blue, black, and green cross symbols indicate Météo-France and UK Met Office (MFUK), National Data Buoy Center (NDBC), TAO (Pacific moorings in black), PIRATA (Atlantic moorings), and RAMA (Indian moorings) (Tropical), and OceanSites buoys, respectively.

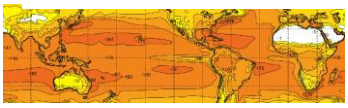

Table 1: Statistics characterizing the comparisons between OceanSites and satellite daily fluxes and bulk variables (10m wind speed (Wspd), 10m specific air humidity (Qa), sea surface temperature (SST), and 10m air temperature (Airt)). They are calculated for all collocated data (1992 – 2017). RMSD, *bs*,and *as* stand for root mean square difference, and linear regression symmetrical intercept and slope coefficients, respectively. The units of the statistical parameters (Mean, STD, RMSD, *bs*, and *as*) associated to LHF, SHF, Wspd, Qa, SST, and Airt, are W/m², W/m², m/s, g/kg, °C, °C, respectively.

	Length	Buoy		RMSD	Correlation	*bs*	*as*
		Mean	STD				
OceanSites Comparisons							
LHF	96485	114.74	60.45	27.73	0.90	0.86	6.83
SHF		6.40	1.98	0.80	0.93	0.98	0.22
Wspd		6.19	2.55	0.97	0.93	0.99	0.41
Qa		15.61	3.79	1.00	0.97	0.99	0.78
SST		25.78	4.83	0.36	1.00	0.99	0.12
Airt		24.67	5.04	0.56	0.99	1.01	-0.67
MFUK Comparisons							
LHF	62547	79.61	59.69	23.45	0.93	0.96	9.45
SHF		15.67	24.21	11.91	0.93	1.22	3.58
Wspd		8.20	3.62	1.66	0.91	1.00	0.17
Qa		8.68	4.16	0.49	0.99	0.99	-0.05
SST		15.54	5.44	0.43	1.00	1.01	-0.11
Airt		14.25	6.03	0.69	0.99	1.04	-0.97
Tropical Comparisons							
LHF	224839	121.36	44.21	24.80	0.86	0.84	7.28
SHF		7.77	6.71	6.24	0.78	1.23	0.73
Wspd		6.40	1.98	0.80	0.93	0.98	0.22
Qa		17.03	1.85	0.79	0.92	0.95	1.34
SST		27.38	1.91	0.36	0.98	0.98	0.36
Airt		26.40	1.81	0.57	0.95	0.96	0.68
NDBC Comparisons							
LHF	252361	103.11	97.57	35.73	0.94	0.83	5.32
SHF		19.89	40.92	13.30	0.95	1.05	1.43
Wspd		6.88	2.93	1.29	0.91	0.99	-0.13
Qa		10.72	5.33	1.11	0.98	1.02	0.25
SST		19.03	7.97	0.67	1.00	0.99	0.34
Airt		17.36	8.60	1.09	0.99	1.02	-0.32

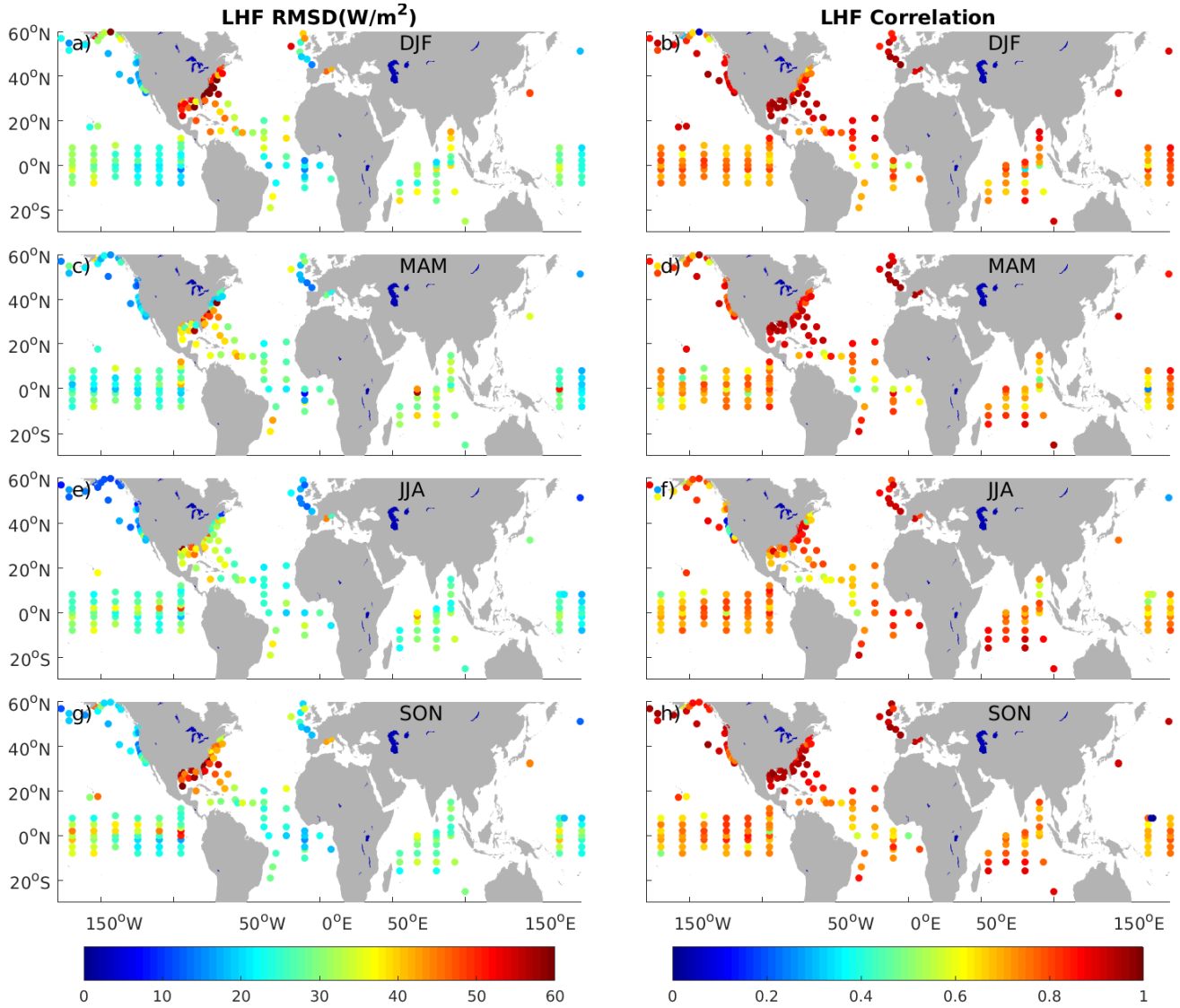

Figure 8: Seasonal distributions of RMSD (left column) and correlation (right column) characterizing the comparison between daily buoy and IFREMER LHF. Panels shown in 1st (top), 2nd, 3rd, and 4th rows relate to the North Hemisphere atmospheric season: winter (December, January, and February (DJF)), spring (March, April, and May (MAM)), summer (June, July, and August (JJA)), and fall (September, October, November (SON)). Colors indicate RMSD (in W/m²), and correlation values.

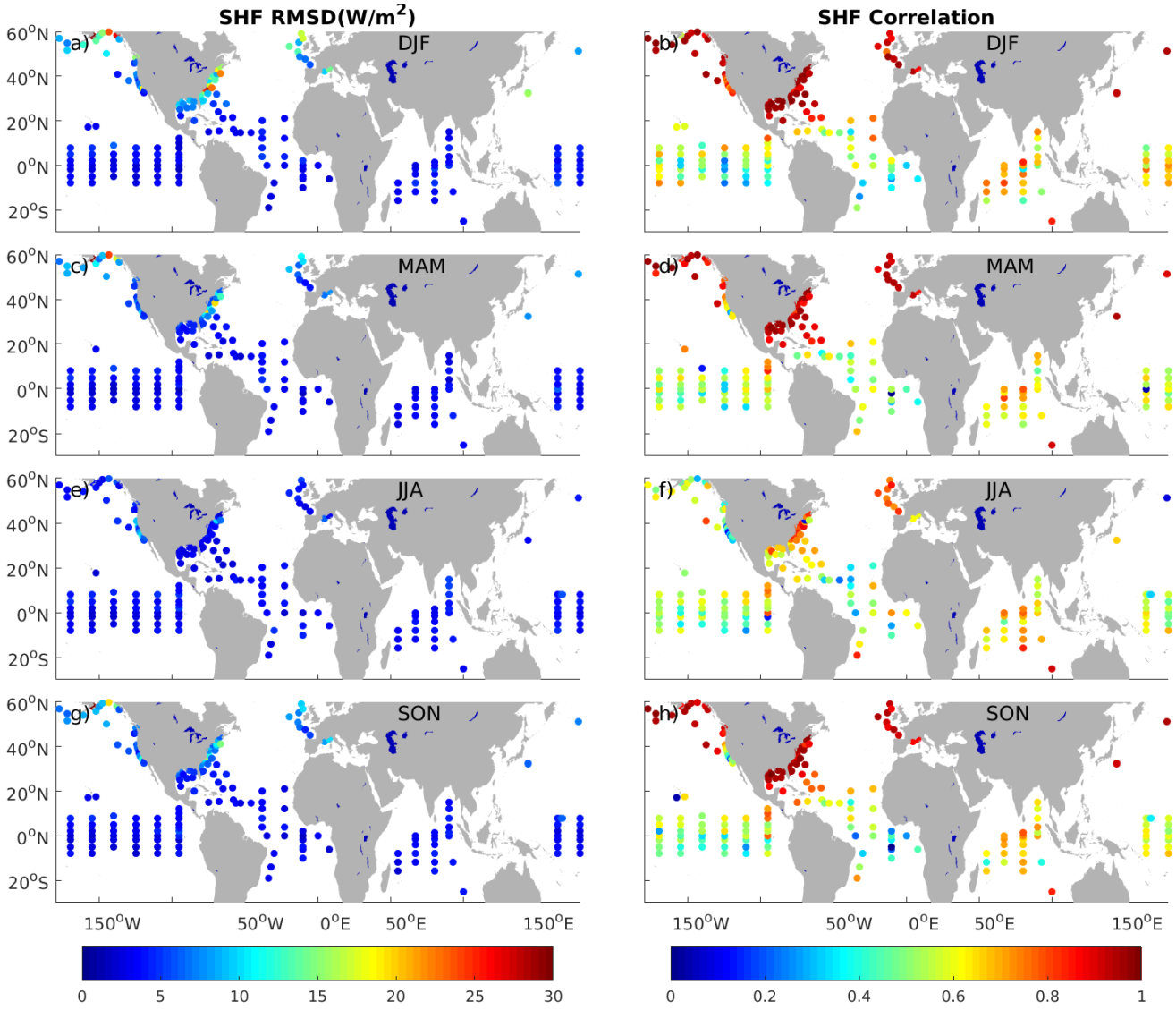

Figure 9: As Figure 7 for SHF

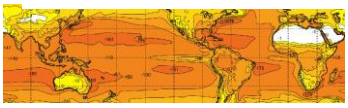

3 Data Access and File Format

Two kind of data are available: daily- and monthly-averaged estimates over global oceans, with regular space grid of 0.25° in latitude and longitude. Files involves turbulent heat fluxes (LHF and SHF), as well as the related bulk variables such as 10m wind speed and the associated wind components, 10m air temperature, sea surface temperature, and 10m specific air humidity.

Data are available through ftp. Login and password would be required. Please contact us for any related information.

ftp://eftp.ifremer.fr/oceanheatflux/data/third-party/fluxes/ifremerflux_v4.1_daily/

ftp://eftp.ifremer.fr/oceanheatflux/data/third-party/fluxes/ifremerflux_v4.1_monthly/

3.1 Daily File

File name: ifremerfluxv4.1_daily-YYYYMMDD120000-OHF-L4-global_daily_0.25x0.25-v0.7-f01.0

YYYY, MM, and DD are year, month, and day, respectively.

File content:

```
        time = UNLIMITED ; // (1 currently)
        lat = 720 ;
        lon = 1440 ;
variables:
        double time(time) ;
                time:long_name = "time" ;
                time:standard_name = "time" ;
                time:units = "days since 1970-01-01 00:00:00Z" ;
        double lat(lat) ;
                lat:long_name = "latitude" ;
                lat:standard_name = "latitude" ;
                lat:authority = "CF-1.8" ;
                lat:units = "degrees_north" ;
        double lon(lon) ;
                lon:long_name = "longitude" ;
                lon:standard_name = "longitude" ;
                lon:authority = "CF-1.8" ;
                lon:units = "degrees_east" ;
        double wind_speed(time, lat, lon) ;
                wind_speed:_FillValue = -32768. ;
                wind_speed:long_name = "wind speed" ;
```

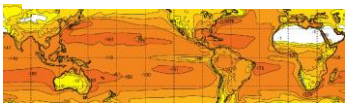

wind_speed:authority = "netCDF 4.3.3.1" ;
wind_speed:units = "m s-1" ;
double eastward_wind(time, lat, lon) ;
eastward_wind:_FillValue = -32768. ;
eastward_wind:long_name = "eastward wind speed" ;
eastward_wind:authority = "netCDF 4.3.3.1" ;
eastward_wind:units = "m s-1" ;
double northward_wind(time, lat, lon) ;
northward_wind:_FillValue = -32768. ;
northward_wind:long_name = "northward wind speed" ;
northward_wind:authority = "netCDF 4.3.3.1" ;
northward_wind:units = "m s-1" ;
double surface_upward_latent_heat_flux(time, lat, lon) ;
surface_upward_latent_heat_flux:_FillValue = -32768. ;
surface_upward_latent_heat_flux:long_name = "surface_upward_latent_heat_flux" ;
surface_upward_latent_heat_flux:authority = "netCDF 4.3.3.1" ;
surface_upward_latent_heat_flux:units = "W m-2" ;
double surface_upward_sensible_heat_flux(time, lat, lon) ;
surface_upward_sensible_heat_flux:_FillValue = -32768. ;
surface_upward_sensible_heat_flux:long_name = "surface_upward_sensible_heat_flux" ;
surface_upward_sensible_heat_flux:authority = "netCDF 4.3.3.1" ;
surface_upward_sensible_heat_flux:units = "W m-2" ;
double sea_surface_temperature(time, lat, lon) ;
sea_surface_temperature:_FillValue = -32768. ;
sea_surface_temperature:long_name = "sea_surface_temperature" ;
sea_surface_temperature:authority = "netCDF 4.3.3.1" ;
sea_surface_temperature:units = "kelvin" ;
double air_temperature(time, lat, lon) ;
air_temperature:_FillValue = -32768. ;
air_temperature:long_name = "air_temperature" ;
air_temperature:authority = "netCDF 4.3.3.1" ;
air_temperature:units = "kelvin" ;
double air_surface_specific_humidity(time, lat, lon) ;
air_surface_specific_humidity:_FillValue = -32768. ;
air_surface_specific_humidity:long_name = "specific_humidity" ;
air_surface_specific_humidity:authority = "netCDF 4.3.3.1" ;
air_surface_specific_humidity:units = "g.kg-1" ;

// global attributes:
:Conventions = "CF-1.8, Unidata Observation Dataset v1.0" ;
:netcdf_version_id = "4.4.1.1 of Mar 8 2019 22:11:53 $" ;
:date_created = "20190524T125235Z" ;
:date_modified = "20190524T125235Z" ;
:id = "FP?" ;
:naming_authority = "fr.ifremer.cersat" ;
:Metadata_Conventions = "Unidata Dataset Discovery v1.0" ;

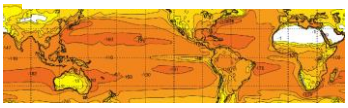

:standard_name_vocabulary = "NetCDF Climate and Forecast (CF) Metadata Convention" ;
:institution = "Ifremer/LOPS-SIAM" ;
:institution_abbreviation = "ifremer/cersat" ;
:title = "Ifremer Daily Satellite global Flux field" ;
:summary = "" ;
:cdm_data_type = "grid" ;
:keywords = "Oceans > Ocean Flux" ;
:keywords_vocabulary = "NASA Global Change Master Directory (GCMD) Science Keywords" ;
:project = "" ;
:acknowledgment = "" ;
:license = "" ;
:format_version = "" ;
:processing_software = "Cersat/Cerbere 1.0" ;
:product_version = "v4.1 (release May 2019)" ;
:uuid = "" ;
:processing_level = "L4" ;
:history = "" ;
:publisher_name = "ifremer/cersat" ;
:publisher_url = "http://cersat.ifremer.fr" ;
:publisher_email = "cersat@ifremer.fr" ;
:creator_name = "" ;
:creator_url = "" ;
:creator_email = "" ;
:references = "e.g. See User Guide and (Bentamy et al, 2013, 2017)" ;
:metadata_link = "" ;
:source = "" ;
:source_version = "" ;
:platform = "" ;
:platform_type = "" ;
:instrument = "" ;
:instrument_type = "" ;
:geospatial_lat_min = -90. ;
:geospatial_lat_max = 89.75 ;
:geospatial_lat_units = "degrees" ;
:geospatial_lat_resolution = 0.25 ;
:geospatial_lon_min = -180. ;
:geospatial_lon_max = 179.75 ;
:geospatial_lon_units = "degrees" ;
:geospatial_lon_resolution = 0.25 ;
:geospatial_vertical_min = "" ;
:geospatial_vertical_max = "" ;
:geospatial_vertical_units = "meters above mean sea level" ;
:geospatial_vertical_positive = "up" ;
:time_coverage_start = "19920101T120000Z" ;
:time_coverage_end = "19920101T120000Z" ;
:time_coverage_resolution = "monthly" ;

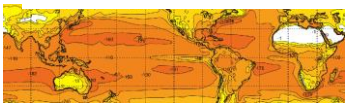

:contact = "abderrahim.bentamy@ifremer.fr, Antoine.Grouazel@ifremer.fr,Jean.Francois.Piolle@ifremer.fr " ;
:easternmost_longitude = "360.f" ;
:grid_resolution = "0.250 degree" ;
:nothernmost_latitude = "90.f" ;
:processing_date = "20190524-12:52:35" ;
:scientific_project = "(OHF) OCEAN-HEAT-FLUX [ESA]" ;
:source_dataset = "FP? converted to OHF standard format" ;
:southernmost_latitude = "-89.75f" ;
:start_time = "19920101T120000Z" ;
:stop_time = "19920101T120000Z" ;
:technical_support_contact = "cersat@ifremer.fr" ;
:westernmost_longitude = "0.25f" ;
}

3.2 Monthly File

File name: `ifremerfluxv4.1_monthly-YYYYMM15120000-OHF-L4-global_monthly_0.25x0.25-v0.7-f01.0`

YYYY and MM are year and month, respectively.

File content:

time = UNLIMITED ; // (1 currently)
lat = 720 ;
lon = 1440 ;
variables:
double time(time) ;
time:long_name = "time" ;
time:standard_name = "time" ;
time:units = "days since 1970-01-01 00:00:00Z" ;
double lat(lat) ;
lat:long_name = "latitude" ;
lat:standard_name = "latitude" ;
lat:authority = "CF-1.8" ;
lat:units = "degrees_north" ;
double lon(lon) ;
lon:long_name = "longitude" ;
lon:standard_name = "longitude" ;
lon:authority = "CF-1.8" ;
lon:units = "degrees_east" ;
double wind_speed(time, lat, lon) ;

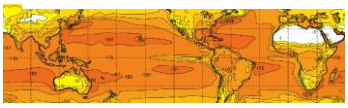

wind_speed:_FillValue = -32768. ;
wind_speed:long_name = "wind speed" ;
wind_speed:authority = "netCDF 4.3.3.1" ;
wind_speed:units = "m s-1" ;
double eastward_wind(time, lat, lon) ;
eastward_wind:_FillValue = -32768. ;
eastward_wind:long_name = "eastward wind speed" ;
eastward_wind:authority = "netCDF 4.3.3.1" ;
eastward_wind:units = "m s-1" ;
double northward_wind(time, lat, lon) ;
northward_wind:_FillValue = -32768. ;
northward_wind:long_name = "northward wind speed" ;
northward_wind:authority = "netCDF 4.3.3.1" ;
northward_wind:units = "m s-1" ;
double surface_upward_latent_heat_flux(time, lat, lon) ;
surface_upward_latent_heat_flux:_FillValue = -32768. ;
surface_upward_latent_heat_flux:long_name =
"surface_upward_latent_heat_flux" ;
surface_upward_latent_heat_flux:authority = "netCDF 4.3.3.1" ;
surface_upward_latent_heat_flux:units = "W m-2" ;
double surface_upward_sensible_heat_flux(time, lat, lon) ;
surface_upward_sensible_heat_flux:_FillValue = -32768. ;
surface_upward_sensible_heat_flux:long_name =
"surface_upward_sensible_heat_flux" ;
surface_upward_sensible_heat_flux:authority = "netCDF 4.3.3.1" ;
surface_upward_sensible_heat_flux:units = "W m-2" ;
double sea_surface_temperature(time, lat, lon) ;
sea_surface_temperature:_FillValue = -32768. ;
sea_surface_temperature:long_name = "sea_surface_temperature" ;
sea_surface_temperature:authority = "netCDF 4.3.3.1" ;
sea_surface_temperature:units = "kelvin" ;
double air_temperature(time, lat, lon) ;
air_temperature:_FillValue = -32768. ;
air_temperature:long_name = "air_temperature" ;
air_temperature:authority = "netCDF 4.3.3.1" ;
air_temperature:units = "kelvin" ;
double air_surface_specific_humidity(time, lat, lon) ;
air_surface_specific_humidity:_FillValue = -32768. ;
air_surface_specific_humidity:long_name = "specific_humidity" ;
air_surface_specific_humidity:authority = "netCDF 4.3.3.1" ;
air_surface_specific_humidity:units = "g.kg-1" ;

// global attributes:
:Conventions = "CF-1.8, Unidata Observation Dataset v1.0" ;
:netcdf_version_id = "4.4.1.1 of Mar 8 2019 22:11:53 $" ;
:date_created = "20190524T152936Z" ;
:date_modified = "20190524T152936Z" ;
:id = "FP?" ;
:naming_authority = "fr.ifremer.cersat" ;

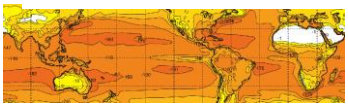

:Metadata_Conventions = "Unidata Dataset Discovery v1.0" ;
:standard_name_vocabulary = "NetCDF Climate and Forecast (CF) Metadata Convention" ;
:institution = "Ifremer/LOPS-SIAM" ;
:institution_abbreviation = "ifremer/cersat" ;
:title = "Ifremer Daily Satellite global Flux field" ;
:summary = "" ;
:cdm_data_type = "grid" ;
:keywords = "Oceans > Ocean Flux" ;
:keywords_vocabulary = "NASA Global Change Master Directory (GCMD) Science Keywords" ;
:project = "" ;
:acknowledgment = "" ;
:license = "" ;
:format_version = "" ;
:processing_software = "Cersat/Cerbere 1.0" ;
:product_version = "v4.1 (release May 2019)" ;
:uuid = "" ;
:processing_level = "L4" ;
:history = "" ;
:publisher_name = "ifremer/cersat" ;
:publisher_url = "http://cersat.ifremer.fr" ;
:publisher_email = "cersat@ifremer.fr" ;
:creator_name = "" ;
:creator_url = "" ;
:creator_email = "" ;
:references = "e.g. See User Guide and (Bentamy et al, 2013, 2017)" ;
:metadata_link = "" ;
:source = "" ;
:source_version = "" ;
:platform = "" ;
:platform_type = "" ;
:instrument = "" ;
:instrument_type = "" ;
:geospatial_lat_min = -90. ;
:geospatial_lat_max = 89.75 ;
:geospatial_lat_units = "degrees" ;
:geospatial_lat_resolution = 0.25 ;
:geospatial_lon_min = -180. ;
:geospatial_lon_max = 179.75 ;
:geospatial_lon_units = "degrees" ;
:geospatial_lon_resolution = 0.25 ;
:geospatial_vertical_min = "" ;
:geospatial_vertical_max = "" ;
:geospatial_vertical_units = "meters above mean sea level" ;
:geospatial_vertical_positive = "up" ;
:time_coverage_start = "19920115T120000Z" ;
:time_coverage_end = "19920115T120000Z" ;
:time_coverage_resolution = "monthly" ;

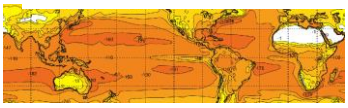

:contact = "abderrahim.bentamy@ifremer.fr, Antoine.Grouazel@ifremer.fr,Jean.Francois.Piolle@ifremer.fr " ;
:easternmost_longitude = "360.f" ;
:grid_resolution = "0.250 degree" ;
:nothernmost_latitude = "90.f" ;
:processing_date = "20190524-15:29:36" ;
:scientific_project = "(OHF) OCEAN-HEAT-FLUX [ESA]" ;
:source_dataset = "FP? converted to OHF standard format" ;
:southernmost_latitude = "-89.75f" ;
:start_time = "19920115T120000Z" ;
:stop_time = "19920115T120000Z" ;
:technical_support_contact = "cersat@ifremer.fr" ;
:westernmost_longitude = "0.25f" ;
}

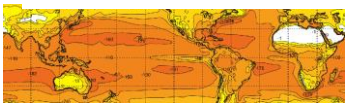

References

Bentamy Abderrahim, Piolle Jean-Francois, Grouazel Antoine, Danielson R., Gulev S., Paul Frederic, Azelmat Hamza, Mathieu P. P., Von Schuckmann Karina, Sathyendranath S., Evers-King H., Esau I., Johannessen J. A., Clayson C. A., Pinker R. T., Grodsky S. A., Bourassa M., Smith S. R., Haines K., Valdivieso M., Merchant C. J., Chapron Bertrand, Anderson A., Hollmann R., Josey S. A. (2017a). **Review and assessment of latent and sensible heat flux accuracy over the global oceans**. *Remote Sensing Of Environment*, 201, 196-218 . http://doi.org/10.1016/j.rse.2017.08.016

Bentamy Abderrahim, Grodsky Semyon A., Elyouncha Anis, Chapron Bertrand, Desbiolles Fabien (2017b). **Homogenization of scatterometer wind retrievals**. *International Journal Of Climatology*, 37(2), 870-889. Publisher's official version: http://doi.org/10.1002/joc.4746 , Open Access version: http://archimer.ifremer.fr/doc/00334/44536/

Bentamy, A., S. A. Grodsky, K. B. Katsaros, A. M. Mestas-Nuñez, B. Blanke and F. Desbiolles (2013): **Improvement in air–sea flux estimates derived from satellite observations**, *International Journal of Remote Sensing*, 34 (14), doi:10.1080/01431161.2013.787502.

Desbiolles Fabien, Bentamy Abderrahim, Blanke Bruno, Roy Claude, Mestas-Nunez Alberto M., Grodsky Semyon A., Herbette Steven, Cambon Gildas, Maes Christophe (2017). **Two Decades [1992-2012] of Surface Wind Analyses based on Satellite Scatterometer Observations**. *Journal Of Marine Systems*, 168, 38-56. Publisher's official version: http://doi.org/10.1016/j.jmarsys.2017.01.003 , Open Access version: http://archimer.ifremer.fr/doc/00366/47686/

Freeman E. and Coauthors, 2017: ICOADS Release 3.0: **A major update to the historical marine climate record**.Int. J. Climatol., 37, 2211–2232, doi:10.1002/joc.4775.

Pinker Rachel T., Bentamy Abderrahim, Zhang Banglin, Chen Wen, Ma Yingtao (2017). **The net energy budget at the ocean-atmosphere interface of the "Cold Tongue" region**. *Journal of Geophysical Research-oceans*, 122(7), 5502-5521. Publisher's official version: http://doi.org/10.1002/2016JC012581 , Open Access version: http://archimer.ifremer.fr/doc/00403/51452/

Wentz F. J., Carl A. Mears, and NOAA CDR Program, 2013: **NOAA Climate Data Record (CDR) of SSM/I and SSMIS Microwave Brightness Temperatures**, RSS Version 7. NOAA National Centers for Environmental Information. doi:10.7289/V5SJ1HKZ [access date].

Wesley D. K. Berg, Mathew R. P. Sapiano, and NOAA CDR Program, 2013: **NOAA Climate Data Record (CDR) of SSM/I and SSMIS Microwave Brightness Temperatures**, CSU Version 1. NOAA National Climatic Data Center. doi:10.7289/V5CC0XMJ

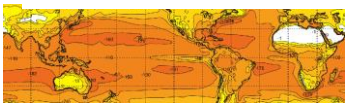

Acknowledgements

The authors are grateful to ESA, CNES, EUMETSAT, CERSAT, JPL, ISRO, CNSA, RSS, ECMWF, Météo-France, UK MetOffice, NDBC, and PMEL for providing satellite, numerical, and in-situ data used in this study. We would like to thank D. Croizé-Fillon and IFREMER/Cersat Team for providing useful processing tools and support. We would like to thank Pr Katsaros who provided useful and relevant comments on the study and manuscript.